Soft Matter

COMMUNICATION

View Article Online
View Journal | View Issue

Check for updates

Cite this: *Soft Matter*, 2017, **13**, 4552

Received 16th March 2017, Accepted 28th May 2017

DOI: 10.1039/c7sm00542c

rsc.li/soft-matter-journal

Avoiding the pull-in instability of a dielectric elastomer film and the potential for increased actuation and energy harvesting

Shengyou Yang,[a] Xuanhe Zhao[bc] and Pradeep Sharma *[ad]

Pull-in instability often occurs when a film of a dielectric elastomer is subjected to an electric field. In this work, we concoct a set of simple, experimentally implementable, conditions that render the dielectric elastomer film impervious to pull-in instability for all practical loading conditions. We show that a uniaxially pre-stretched film has a significantly large actuation stretch in the direction perpendicular to the pre-stretch and find that the maximal specific energy of a dielectric elastomer generator can be increased from 6.3 J g^{-1} to 8.3 J g^{-1} by avoiding the pull-in instability.

Soft dielectrics are capable of achieving significantly large deformations and find application in humanlike robots,[1,2] stretchable electronics,[3] actuators,[4–6] and energy harvesters[7–11] among others.[12,13] However, soft dielectrics under applied electric fields are also vulnerable to various types of electromechanical instabilities.[14–19] Instabilities are often thought to be detrimental to material and device functionality and often avoided by design. Recent works have, however, focused on harnessing instabilities for various applications such as artificial muscles,[20,21] dynamic surface patterning,[22,23] giant voltage-triggered deformation,[24,25] and energy harvesting.[26,27]

A commonly used actuator is a dielectric thin film coated with two compliant electrodes. Upon application of a potential difference between the two electrodes, the dielectric film thins down in the thickness direction and expands laterally. When the thickness decreases to a certain threshold, the film is unable to sustain the electric field and the so-called pull-in instability occurs.[14–16,26,28] To avoid failure and to enhance the actuation strain and the harvested electrical energy density, pull-in instability is often suppressed by using a pre-stress,[28] materials that exhibit load-dependent stiffening[29,30] and charge-controlled operation.[6,31] Moreover, pull-in instability can also be delayed or eliminated by pre-stretch.[32–34] In this work we analyze how properly chosen (and experimentally realizable) boundary conditions can be exploited to avoid or delay pull-in instability. We show that the pull-in instability can be summarily avoided by a judicious combination of dead-loads and controlled-displacement boundary conditions which renders the pertinent Hessian matrix of the equilibrium state positive-definite under all practical conditions. By prevention of pull-in instability and through exploitation of the competition between various pertinent factors such as electromechanical loading conditions, consideration of buckling, and pre-stretch, among others, we theoretically highlight a significantly increased ability for energy harvesting and actuation. However, realizing the theoretical maximum energy conversion experimentally has still remained elusive and the reduction of the disparity between experiments and theoretical predictions appears to be a challenging task.[7–10]

Consider an elastic dielectric film with dimensions (L_1, L_2, L_3) in its undeformed state. Subjected to the voltage Φ and the dead load P_2 at a prescribed stretch λ_1, the incompressible film deforms to a homogeneous state with stretches λ_1, λ_2, and $\lambda_3 = \lambda_1^{-1}\lambda_2^{-1}$. Moreover, the film gains a magnitude of total charge Q that distributes uniformly on either side of the compliant electrodes. The homogeneously deformed film is shown in Fig. 1. We remark that the loading device actually controls the normal displacement (or the stretch λ_1) only on the two sides of the film in the X_1 direction. Since the deformation is homogeneous under these circumstances, the entire film exhibits prescribed stretch λ_1.

The nominal electric field and the nominal electric displacement are defined as $\tilde{E} = \Phi/L_3$ and $\tilde{D} = Q/L_1L_2$, respectively. The true electric field and the electric displacement are defined as $E = \Phi/(\lambda_3L_3)$ and $D = \lambda_3Q/(L_1L_2)$. Furthermore, the nominal and true stresses from the dead load P_2 are denoted, respectively, as $s_2 = P_2/(L_1L_3)$ and $\sigma_2 = \lambda_2P_2/(L_1L_3)$.

The free energy of the system is[28,35]

$$G = L_1L_2L_3W(\lambda_1,\lambda_2,\tilde{D}) - P_2\lambda_2L_2 - \Phi Q. \tag{1}$$

[a] Department of Mechanical Engineering, University of Houston, Houston, TX 77204, USA
[b] Department of Mechanical Engineering, Massachusetts Institute of Technology, Cambridge, MA 02139, USA
[c] Department of Civil and Environmental Engineering, Massachusetts Institute of Technology, Cambridge, MA 02139, USA
[d] Department of Physics, University of Houston, Houston, TX 77204, USA. E-mail: psharma@uh.edu; Fax: +1-713-743-4503; Tel: +1-713-743-4502

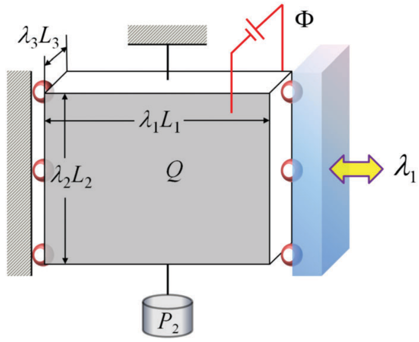

Fig. 1 Schematic diagram of a deformed film of a dielectric elastomer. The film is extended/compressed between two well-lubricated (with rollers), rigid plates by means of a controlled displacement (or the stretch λ_1) in the X_1 direction. A dead load P_2 is applied in the X_2 direction and a voltage Φ is applied in the thickness direction of the film that is coated with two compliant electrodes. The loads deform the film from L_1, L_2, and L_3 to $\lambda_1 L_1$, $\lambda_2 L_2$, and $\lambda_3 L_3$, as well as induce an electric charge of magnitude Q on either electrode.

We remark that the stretch λ_1, the dead load P_2, and the voltage Φ in eqn (1) are prescribed parameters. In contrast to Yang *et al.*[36] and Dorfmann and Ogden[37] the dielectric film in this work admits only a class of homogeneous deformations. Thus, the general coordinate λ_1 has a zero variation $\delta\lambda_1 = 0$ for any homogeneous perturbation. When other two generalized coordinates λ_2 and $\tilde{D}$ vary by small amounts $\delta\lambda_2$ and $\delta\tilde{D}$, the free energy of the system varies by

$$\begin{aligned}\frac{\delta G}{L_1 L_2 L_3} &= \left(\frac{\partial W}{\partial \lambda_2} - s_2\right)\delta\lambda_2 + \left(\frac{\partial W}{\partial \tilde{D}} - \tilde{E}\right)\delta\tilde{D} \\ &\quad + \frac{1}{2}\frac{\partial^2 W}{\partial \lambda_2^2}\delta\lambda_2^2 + \frac{1}{2}\frac{\partial^2 W}{\partial \tilde{D}^2}\delta\tilde{D}^2 + \frac{\partial^2 W}{\partial\lambda_2\partial\tilde{D}}\delta\lambda_2\delta\tilde{D},\end{aligned} \tag{2}$$

where only the first and second variations are retained and all the high-order terms are omitted. At equilibrium, the first variation vanishes, and yields the following equilibrium equations:

$$s_2 = \frac{\partial W}{\partial \lambda_2}, \quad \tilde{E} = \frac{\partial W}{\partial \tilde{D}}, \tag{3}$$

where the nominal stress $s_2 = P_2/(L_1 L_3)$ and the nominal electric field $\tilde{E} = \Phi/L_3$ are prescribed parameters. In contrast, the nominal stress s_1 is defined as

$$s_1 = \frac{\partial W}{\partial \lambda_1}, \tag{4}$$

which is no longer prescribed but depends on λ_2 and $\tilde{D}$ as well as λ_1. Indeed, the partial derivative in eqn (4) is to be understood as the partial derivative of W with respect to λ_1 at the prestretch λ_1. It is exactly the coefficient of the zero $\delta\lambda_1$ in the first variation of the energy. Thus, it has been omitted in the variation form for simplicity. In equilibrium, from Cauchy's stress theorem, s_1 in eqn (4) is equal to the stress generated by the force applied on the left and right surfaces, and the magnitude of the force is $s_1 L_2 L_3$.

From the principle of minimum energy, the stability of the equilibrium solution requires a positive-definite second variation in eqn (2) for arbitrary $\delta\lambda_2$ and $\delta\tilde{D}$, that is, the Hessian matrix

$$\mathbf{H} = \begin{bmatrix} \dfrac{\partial^2 W}{\partial \lambda_2^2} & \dfrac{\partial^2 W}{\partial\lambda_2\partial\tilde{D}} \\ \dfrac{\partial^2 W}{\partial\lambda_2\partial\tilde{D}} & \dfrac{\partial^2 W}{\partial \tilde{D}^2} \end{bmatrix} \tag{5}$$

must be positive definite for the equilibrium solution.

Consider an ideal dielectric elastomer with the free energy function,[28,35]

$$W(\lambda_1, \lambda_2, \tilde{D}) = \frac{\mu}{2}(\lambda_1^2 + \lambda_2^2 + \lambda_1^{-2}\lambda_2^{-2} - 3) + \frac{\tilde{D}^2}{2\varepsilon}\lambda_1^{-2}\lambda_2^{-2}, \tag{6}$$

where μ is the small-strain shear modulus and ε is the permittivity. The first and second terms on the right-hand side of eqn (6) are the elastic and the dielectric energy. Then the equilibrium condition [eqn (3)] and the nominal stress s_1 in eqn (4) become

$$s_2 = \mu\left[\lambda_2 - \left(1 + \frac{\tilde{D}^2}{\varepsilon\mu}\right)\lambda_1^{-2}\lambda_2^{-3}\right], \tag{7a}$$

$$\tilde{E} = \frac{\tilde{D}}{\varepsilon}\lambda_1^{-2}\lambda_2^{-2}, \tag{7b}$$

and

$$s_1 = \mu\left[\lambda_1 - \left(1 + \frac{\tilde{D}^2}{\varepsilon\mu}\right)\lambda_1^{-3}\lambda_2^{-2}\right]. \tag{8}$$

Eqn (7) contains two algebraic equations with two variables λ_2 and $\tilde{D}$ and three prescribed parameters λ_1, s_2, and $\tilde{E}$. A quartic equation in terms of λ_2 can be obtained by eliminating $\tilde{D}$, such that

$$(\mu - \lambda_1^2\varepsilon\tilde{E}^2)\lambda_2^4 - s_2\lambda_2^3 - \mu\lambda_1^{-2} = 0, \tag{9}$$

which has only one positive real root of λ_2 if and only if

$$0 \le \frac{\tilde{E}}{\sqrt{\mu/\varepsilon}} < \lambda_1^{-1}, \tag{10}$$

and the real root of λ_2 in eqn (9) is a real number between max $\{s_2(\mu - \lambda_1^2\varepsilon\tilde{E}^2)^{-1}, \mu^{1/4}\lambda_1^{-1/2}(\mu - \lambda_1^2\varepsilon\tilde{E}^2)^{-1/4}\}$ and their sum. Hence the critical nominal electric field is given by

$$\frac{\tilde{E}^*}{\sqrt{\mu/\varepsilon}} = \lambda_1^{-1} \tag{11}$$

below which the equilibrium solution can exist. We note that under the condition [eqn (10)] with prescribed parameters $\lambda_1 > 0$, $s_2 \ge 0$, and $\tilde{E} \ge 0$, eqn (7) exhibits positive solutions for λ_2 and $\tilde{D}$. Otherwise, eqn (7) has no solution for realistic physical situations that admit positive λ_2 and non-negative $\tilde{D}$.

The electromechanical stability of the electrostatic system directly relates to the property of the Hessian matrix [eqn (5)] that, at equilibrium [eqn (7)], is given by

$$\mathbf{H} = \begin{bmatrix} \mu\left[1+3\left(1+\frac{\tilde{D}^2}{\varepsilon\mu}\right)\lambda_1^{-2}\lambda_2^{-4}\right] & -\frac{2\tilde{D}}{\varepsilon}\lambda_1^{-2}\lambda_2^{-3} \\ -\frac{2\tilde{D}}{\varepsilon}\lambda_1^{-2}\lambda_2^{-3} & \frac{1}{\varepsilon}\lambda_1^{-2}\lambda_2^{-2} \end{bmatrix}. \quad (12)$$

The 1×1 principal minors of the Hessian matrix [eqn (12)] are the diagonal entries $\mathbf{H}_{11} > 0$ and $\mathbf{H}_{22} > 0$, and the only 2×2 principal minor is the determinant of the Hessian matrix [eqn (12)], which is always positive, namely

$$\det \mathbf{H} = \frac{1}{\varepsilon}\lambda_1^{-4}\lambda_2^{-6}\left(4\mu + s_2\lambda_1^2\lambda_2^3\right) > 0 \quad (13)$$

due to the fact that $s_2 = P_2/(L_1L_3) \geq 0$. Since all principal minors are positive, the Hessian matrix $\mathbf{H}$ [eqn (12)] is always positive-definite. A positive-definite Hessian matrix ensures the stability of the homogeneous deformation in equilibrium, because the dielectric film in equilibrium is in a state of minimum free-energy. Thus the pull-in instability never appears in this homogeneously deformed system loaded with a prescribed stretch, a dead load and an electric voltage under the condition [eqn (10)]. We emphasize that the stability is under the condition that the film is not buckled in the X_1 direction—we will return to this point later in the communication.

To further understand the behavior of the dielectric film in equilibrium, two special cases are discussed. Case I is a dielectric film at a prescribed stretch $\lambda_1 = 1$ under an electric field and several dead loads s_2, while case II is a dielectric film at a zero dead load $s_2 = 0$ under an electric field and several prescribed stretches λ_1.

In Fig. 2, we plot the behavior of the dielectric film for case I, *i.e.* $\lambda_1 = 1$. Fig. 2(a) shows that the nominal electric field increases monotonically with the increase of the nominal electric displacement. The nominal electric field is bounded by eqn (11) and the critical nominal electric field for the nonexistence of equilibrium solutions at $\lambda_1 = 1$ is $\tilde{E}^*\sqrt{\varepsilon/\mu} = 1$. With a constant nominal electric field but an increase of the dead load s_2, the nominal electric displacement increases in Fig. 2(a), since a dead load leads to a reduced thickness but a larger area, thus resulting in a larger capacity (and charge). Fig. 2(b) shows the relation of the nominal electric displacement and the true electric field under several dead loads s_2.

In Fig. 2(c), the variation of the stretch λ_2 is plotted. Both the nominal electric field and the dead load s_2 can increase the stretch λ_2. At the critical value $\tilde{E}^*\sqrt{\varepsilon/\mu} = 1$, the stretch λ_2 increases to infinity and the thickness ($\lambda_3 = \lambda_2^{-1}$) decreases to zero, which, of course, is impossible in reality since prior to such a blowup, electric breakdown will ensue due to the large true electric field or, alternatively, mechanical rupture will take place. The actuation stretch is defined as λ_2/λ_{2p}, where λ_{2p} is the pre-stretch that exists due to the prescribed stretch λ_1 and the dead load s_2. At a prescribed stretch $\lambda_1 = 1$, the actuation stretch λ_2/λ_{2p} under several dead loads s_2 is shown in Fig. 2(d).

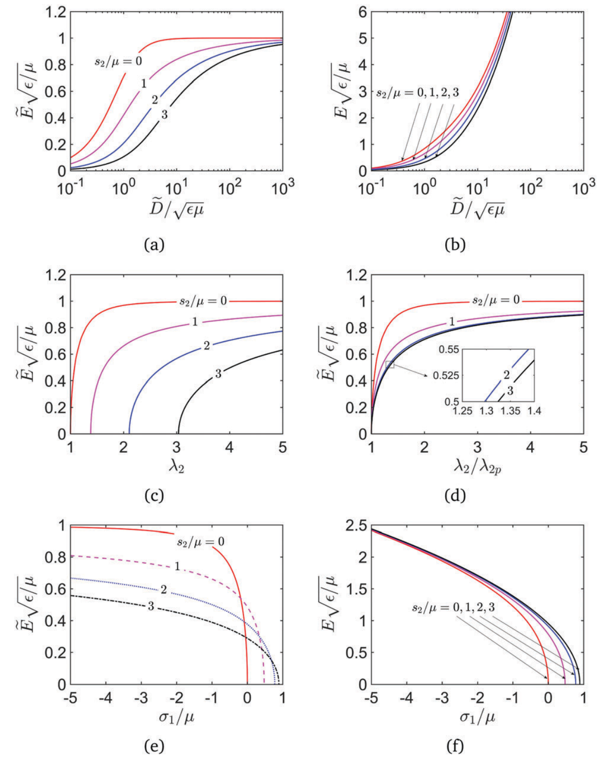

Fig. 2 Behavior of the neo-Hookean dielectric film at $\lambda_1 = 1$ under various loads, s_2/μ: (a) nominal electric displacement *vs.* nominal electric field, (b) nominal electric displacement *vs.* true electric field, (c) stretch λ_2 *vs.* nominal electric field, (d) actuation stretch λ_2/λ_{2p} *vs.* nominal electric field, (e) true stress *vs.* nominal electric field, and (f) true stress *vs.* true electric field.

The true stress $\sigma_1 = \lambda_1 s_1$ shown in Fig. 2(e) is directly related to electrical buckling and will be analyzed in the following. At a zero dead load in Fig. 2(e), the true stress is $\sigma_1/\mu = 1 - (1 - \varepsilon\tilde{E}^2/\mu)^{-1/2}$, and the nominal electric field induces a compressive state in the film, *i.e.* $\sigma_1 < 0$, and the magnitude $|\sigma_1|$ increases monotonically with the increase of the nominal electric field. On the other hand, at a zero electric field, a dead load s_2 expands the film ($\lambda_2 > 1$) and induces a tensile state *i.e.* $\sigma_1/\mu = 1 - \lambda_2^{-2} > 0$ in Fig. 2(e). Interestingly, there exists a competition between the electric field and the dead load due to their opposite effects on the stress σ_1. At a low electric field, the dead load makes the dielectric film extend within the plane. When the electric field increases, the stress σ_1 gradually decreases from a tensile stress ($\sigma_1 > 0$) to a compressive one ($\sigma_1 < 0$). Without considering electric breakdown (under a high true electric field) and rupture by stretch (at a high stretch λ_2), the continually increasing $|\sigma_1|$ of the compressive stress will finally make the dielectric film buckle.

Fig. 3 plots the behavior of the dielectric film for case II, *i.e.* $s_2 = 0$. We note that eqn (11) gives the limit of the nominal electric field, for example, $\tilde{E}^*\sqrt{\varepsilon/\mu} = 1$ for a prescribed stretch $\lambda_1 = 1$, while it is 0.2 for $\lambda_1 = 5$ in Fig. 3(a), (c) and (e). The increase of the stretch λ_1 in Fig. 3(a) increases the film surface area, leading to higher capacity and gain of additional charge.

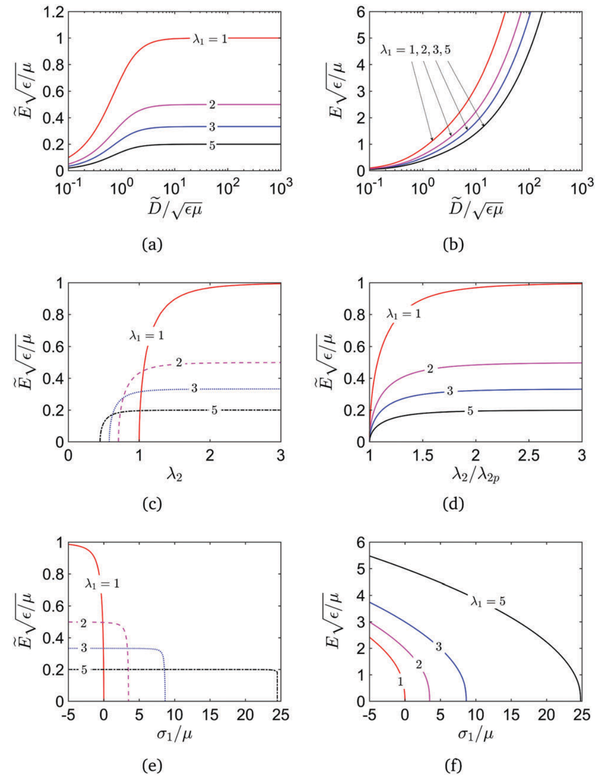

Fig. 3 Behavior of a neo-Hookean dielectric film at $s_2 = 0$ under various stretches λ_1: (a) nominal electric displacement *vs.* nominal electric field, (b) nominal electric displacement *vs.* true electric field, (c) stretch λ_2 *vs.* nominal electric field, (d) actuation stretch λ_2/λ_{2p} *vs.* nominal electric field, (e) true stress *vs.* nominal electric field, and (f) true stress *vs.* true electric field.

In other words, at a prescribed nominal electric field below $\tilde{E}^*\sqrt{\varepsilon/\mu}$, a larger stretch λ_1 corresponds to a higher nominal electric displacement. Fig. 3(b) shows the corresponding relation between the true electric field and the nominal electric displacement.

In Fig. 3(c), the increase of the stretch λ_1 in the length direction will make the film decrease its width (or the pre-stretch λ_{2p} at a zero electric field), pre-stretch but an electric field, on the other hand, will tend to make the film expand in-plane and exhibit a larger stretch (λ_2). At $s_2 = 0$, the actuation stretch λ_2/λ_{2p} under several prescribed stretches λ_1 is shown in Fig. 3(d).

The true stress from eqn (7) and (8) at $s_2 = 0$ is obtained as $\sigma_1/\mu = \lambda_1 s_1/\mu = \lambda_1{}^2 - \lambda_1{}^{-1}(1 - \lambda_1{}^2\varepsilon\tilde{E}^2/\mu)^{-1/2}$. Without the electric field, the true stress σ_1/μ is $\lambda_1{}^2 - \lambda_1{}^{-1}$. When the electric field increases from zero, for example, at a prescribed stretch $\lambda_1 > 1$ in Fig. 3(e) and (f), the true stress σ_1 will decrease from a tensile stress ($\sigma_1 > 0$) to a compressive one ($\sigma_1 < 0$).

It is well-known that a thin film subjected to a lateral compression is easy to buckle. In our model, the deformation in the X_1 direction is controlled by two well-lubricated plates, and a compressive stress ($\sigma_1 < 0$) in the film can occur under some conditions (see Fig. 2(e), f, 3e and f for example). In the following, we will discuss electric buckling of a dielectric film subjected to electromechanical loads.

The special case, loss of tension, is of interest because it is a turning point for the compression–tension behavior of the dielectric film. The compressive stress can make the film buckle and should be avoided.[5,7,36,37] When the nominal stress s_1 in eqn (8) becomes zero, it is in the so-called state of loss of tension. From the equilibrium equations [eqn (7)], the nominal electric field at loss of tension is

$$\frac{\tilde{E}^{\mathrm{c}}}{\sqrt{\mu/\varepsilon}} = \lambda_2{}^{-1}\sqrt{1 - \lambda_1{}^{-4}\lambda_2{}^{-2}} \quad \text{for } \lambda_1{}^2\lambda_2 \geq 1, \tag{14}$$

where $\lambda_2 = \dfrac{1}{2\mu}\left(s_2 + \sqrt{s_2{}^2 + 4\mu^2\lambda_1{}^2}\right) \geq \lambda_1$ due to $s_2 = P_2/(L_1L_3) \geq 0$.

At the state of loss of tension, if we, for example, continue to prescribe the stretch λ_1 and the dead load s_2 but increase the nominal electric field, the stress s_1 in eqn (8) will decrease from zero to negative and the film will be in a state of compression. Inspired by Euler's buckling of a long, slender, ideal column, we analyze here the electrical buckling of a dielectric film. Euler's formula for the buckling of a column with two fixed end supports is

$$F^{\mathrm{c}} = \frac{4\pi^2 E^{\mathrm{e}} I^{\mathrm{e}}}{L_1{}^2}, \tag{15}$$

where F^{c} is the critical compressive force, E^{e} is the effective elastic modulus, I^{e} is the area moment of inertia of the cross section, and L_1 is the length of the column. For a film of an incompressible neo-Hookean dielectric with shear modulus μ under the small-deformation assumption, the effective modulus is $E^{\mathrm{e}} = 3\mu$ and $I^{\mathrm{e}} = L_3{}^3L_2/12$. Thus the critical compressive stress f^{c} from eqn (15) is

$$f^{\mathrm{c}} = \mu\bar{f}^{\mathrm{c}} = \frac{F^{\mathrm{c}}}{L_2L_3} = \frac{\mu\pi^2}{(L_1/L_3)^2}. \tag{16}$$

It is assumed that the dielectric film begins to buckle when the magnitude of the compressive stress $\sigma_1 = \lambda_1 s_1 < 0$ in eqn (8) reaches f^{c} in eqn (16). Together with the equilibrium equations [eqn (7)], the critical nominal electric field for the electrical buckling can be expressed as

$$\frac{\tilde{E}^{\mathrm{c}}}{\sqrt{\mu/\varepsilon}} = \lambda_2{}^{\mathrm{c}-1}\sqrt{1 + \bar{f}^{\mathrm{c}}\lambda_1{}^{-2} - \lambda_1{}^{-4}\lambda_2{}^{\mathrm{c}-2}}, \tag{17}$$

where $\lambda_2^{\mathrm{c}} = \dfrac{1}{2\mu}\left(s_2 + \sqrt{s_2{}^2 + 4\mu^2(\lambda_1{}^2 + \bar{f}^{\mathrm{c}})}\right)$ and $\bar{f}^{\mathrm{c}} = \pi^2/(L_1/L_3)^2$. Compared with the length (L_1) and the width (L_2) of the film, the thickness (L_3) is often much smaller. Then the buckling stress $\bar{f}^{\mathrm{c}}$ in eqn (16) is very small, for example, $\bar{f}^{\mathrm{c}} < 0.1$ for a film with an aspect ratio $L_1/L_3 > 10$. Therefore, the critical nominal electric field in eqn (17) for buckling is very close to that in eqn (14) for the loss of tension.

Fig. 4 shows the critical electric fields for the loss of tension [eqn (14)] and electrical buckling [eqn (17)] in which the aspect ratio is chosen to be $L_1/L_3 = 10$. The difference between the two

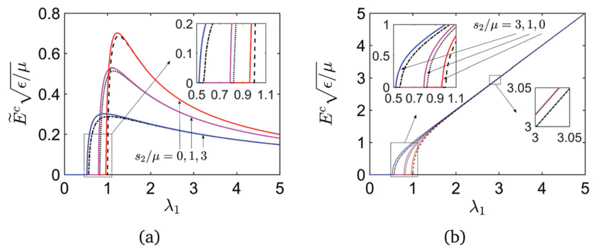

Fig. 4 Comparison of the loss of tension (dashed lines) and electrical buckling (solid lines) under several dead loads s_2/μ. Effects of the stretch λ_1 on (a) the critical nominal electric field and (b) the critical true electric field.

critical nominal electric fields is negligible at a stretch $\lambda_1 > 1$, while it is minor at a stretch $\lambda_1 < 1$. Moreover, the critical electric field for the loss of tension is always below that of electrical buckling. Therefore, there is no electrical buckling when a loss of tension occurs in the film, but the film will buckle if the electric field increases.

For each curve in Fig. 4(a), there exists a peak that corresponds to the maximum of the critical nominal electric field. At that peak, any infinitesimal variation of the stretch λ_1 will make the film buckle; however, the decrease of the nominal electric field will avoid the electrical buckling. On the other hand, if a point on the buckling curve is on the left-hand side of the peak, the increase of the stretch λ_1 will avoid the electrical buckling, while a point is on the right-hand side of the peak, the electrical buckling can be avoided by a decrease of the stretch λ_1. The corresponding relation between the critical true electric field and the stretch λ_1 is shown in Fig. 4(b).

A high actuation strain for an actuator driven by an electric field is desirable. Without an electric field, the pre-stretch λ_{2p} due to the prescribed stretch λ_1 and the dead load s_2 can be determined by eqn (7) with $\tilde{E} = 0$. The effects of s_2 and λ_1 on the pre-stretch λ_{2p} are shown in Fig. 5(a). The pre-stretch is $\lambda_{2p} = \lambda_1{}^{-1/2}$ at $s_2 = 0$, while it is approximately equal to s_2/μ at a high dead load.

Subjected to the electric field, the dielectric film thins down and expands in the plane. When the electric field increases to the critical value in eqn (17), the electrical buckling occurs in the dielectric film with a critical stretch $\lambda_2{}^c$. The critical actuation stretch is defined as λ_2^c/λ_{2p}. Fig. 5(b) plots the effects of the stretch λ_1 and the dead load s_2 on the actuation stretch λ_2^c/λ_{2p}.

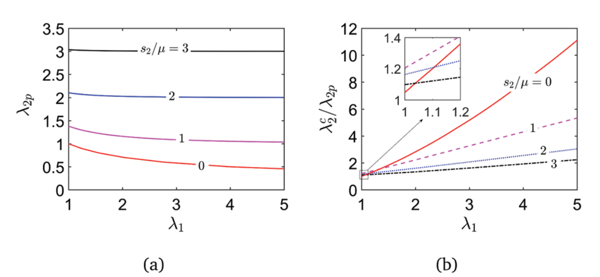

Fig. 5 Effects of the prescribed stretch λ_1 and the dead load s_2 on (a) the pre-stretch λ_{2p} and (b) the critical actuation stretch λ_2^c/λ_{2p}.

It shows that when the dielectric film is subjected to a prescribed stretch λ_1, the actuation stretch in the direction normal to the prescribed stretch is significantly larger, especially in the case of a larger prescribed stretch (λ_1) and at a zero dead load ($s_2 = 0$). Hence the actuation stretch can be dramatically increased by a prescribed stretch. A similar observation has also reported before in the analysis of the electromechanical instability of a uniaxial pre-stressed dielectric film.[28]

Inspired by the aforementioned discussion related to the avoidance of pull-in instability, we now show the possibility of increasing the capacity of the energy conversion of a dielectric elastomer generator. It is known that the usual modes of failure in a dielectric film include electrical breakdown (EB), electromechanical instability (EMI or pull-in instability), loss of tension, and rupture by stretch. The area of the cycle enclosed by these four modes of failure is exactly the maximal energy that can be converted in a dielectric film subjected to equal biaxial in-plane forces.[7] With the same dielectric film but mechanical boundary conditions suggested in this work, the pull-in instability can be avoided and then the four modes of failure reduce to three. This reduction admits the possibility of enhanced energy conversion. In the following, we will show that not only the maximal energy of a dielectric elastomer generator but also the specific energy enclosed by a rectangular in the voltage–charge plane and the amplification of voltage (ratio of the input voltage to the output voltage) can be increased significantly.

In a previous work,[7] the dielectric film is subjected to equal biaxial in-plane forces and voltage in the thickness direction, such that the equal nominal stresses $s_1 = s_2$ and the equal stretches $\lambda_1 = \lambda_2$ at equilibrium. It should be noted that there is no difference between the forms of the equilibrium equations in the work[7] and in this paper, but the difference is the control parameters. Unlike the equal biaxial in-plane forces,[7] this paper takes a prescribed stretch λ_1 and a dead load s_2 as control parameters. Since the equilibrium equations have the same forms, the equilibrium solutions of a film subjected to equal biaxial in-plane forces – as discussed by Koh *et al.*[7] – can be achieved by choosing properly controlled parameters (λ_1, s_2) in this work; however, the pull-in instability will be avoided. This similarity makes feasible the direct use of their model in this work for the illustration of enhanced energy conversion by the proposed avoidance of the pull-in instability.

To make this communication self-contained, we briefly review the four modes of failure when subjected to equal nominal stresses $s = s_1 = s_2$ and equal stretches $\lambda = \lambda_1 = \lambda_2$ in equilibrium [eqn (7)]. First, the curve under a zero electric field ($E = 0$) in Fig. 6(a) is determined by eqn (7a) with $\tilde{D} = 0$, while it is the origin in Fig. 6(b). Next, the electrical breakdown (EB) curve is governed by eqn (7) with $\tilde{E} = E_{EB}\lambda^{-2}$, where $E_{EB} = 3 \times 10^8$ V m^{-1} is the critical true electric field when EB occurs.[7,38] Other material parameters used in the numerical calculations are $\mu = 10^6$ N m^{-2} and $\varepsilon = 3.54 \times 10^{-11}$ F m^{-1} as well as the mass density $\rho = 1000$ kg m^{-3}. Then, the curve of the loss of tension is the horizontal axis in Fig. 6(a), while it is represented by eqn (7) with $s = 0$ in Fig. 6(b). The curve of rupture by stretch in Fig. 6(a) is the vertical line $\lambda = \lambda_R$ while in Fig. 6(b) it is

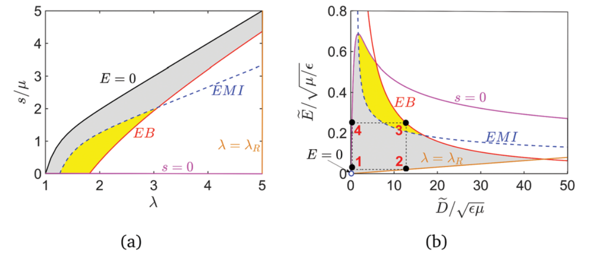

Fig. 6 A thermodynamic state of the dielectric film is represented by (a) a point in the force–displacement plane or (b) a point in the voltage–charge plane. The equilibrium curve under the zero electric field is denoted as $E = 0$. Four modes of failure including EB, EMI, loss of tension $s = 0$, and rupture by stretch $\lambda = \lambda_R$ are also plotted.

determined by eqn (7b) with $\lambda = \lambda_R$, where $\lambda_R \leq 6$ when the film ruptures when subjected to equal biaxial stretch.[15] Here we use $\lambda_R = 5$. Last, the curve of electromechanical instability (EMI) is based on eqn (6) and (7) in the work by Koh *et al.*[7]

In Fig. 6, the shaded areas enclosed by various modes of failure (also the $E = 0$ curve) define the maximal energy of conversion, that is, the maximal specific energy. In the work by Koh *et al.*[7] four modes of failure leads to a maximal specific energy of 6.3 J g^{-1}. In contrast, the EMI (pull-in instability) is avoided in our proposed scheme and the remaining three modes of failure admit a maximal specific energy of 8.3 J g^{-1}, increasing the capacity of the dielectric elastomer generator by nearly 33%.

The aforementioned maximal-energy cycle is idealized and may be difficult to realize in practice. The rectangular[7] and triangular[39] cycles are often used for energy conversion. We refer the reader to the Koh *et al.*[7,39] for the detailed circuit design that pumps electric charge from a low-voltage battery to a high-voltage battery. A rectangle with vertices 1–2–3–4 is plotted in Fig. 6(b), where the energy enclosed by the rectangle is called the specific energy. The electric voltage corresponding to vertices (1,2) is the input voltage Φ_{in}, while the electric voltage corresponding to vertices (3,4) is the output voltage Φ_{out}. The specific energy and the amplification of voltage for various Φ_{in} are plotted in Fig. 7(a) and (b). Evidently, the avoidance of pull-in instability can enhance the ability of energy conversion of a dielectric elastomer generator by increasing the specific energy and the voltage amplification.

In summary, in this work, we propose the avoidance of the pull-in instability of a dielectric film by introducing controlled-displacement boundary conditions, which ensure that the Hessian matrix is always positive definite in equilibrium regardless of the values assigned to the prescribed stretch, the dead load, and the electric field. The limit of the nominal electric field for the existence of equilibrium solutions is presented. We also show that the critical electric field for the loss of tension is slightly below that of electrical buckling and a uniaxial pre-stretched dielectric film can exhibit a significantly larger actuation strain in the direction perpendicular to the pre-stretch. Here we should emphasize that the film needs to be highly pre-stretched, uniaxially, to avoid loss of tension (or electrical buckling) when the electric field is high and the dead load is low. Finally, we find that the maximal specific energy that can be harvested may be increased from 6.3 J g^{-1} to 8.3 J g^{-1} by avoiding pull-in instability.

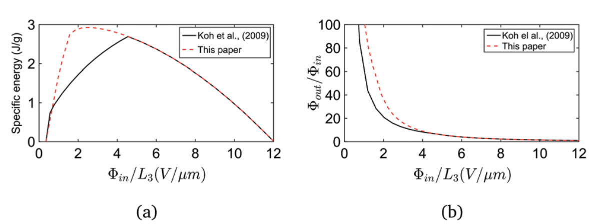

Fig. 7 Specific energy (a) and amplification of voltage (b) for cycles represented by various rectangles in Fig. 6(b).

Acknowledgements

The authors gratefully acknowledge support from NSF CMMI Grant No. 1463205 and the M. D. Anderson Professorship.

References

1 N. Lu and D.-H. Kim, *Soft Robotics*, 2014, **1**, 53–62.
2 S. Shian, K. Bertoldi and D. R. Clarke, *Adv. Mater.*, 2015, **27**, 6814–6819.
3 J. A. Rogers, T. Someya and Y. Huang, *Science*, 2010, **327**, 1603–1607.
4 R. Shankar, T. K. Ghosh and R. J. Spontak, *Soft Matter*, 2007, **3**, 1116–1129.
5 M. Moscardo, X. Zhao, Z. Suo and Y. Lapusta, *J. Appl. Phys.*, 2008, **104**, 093503.
6 C. Keplinger, M. Kaltenbrunner, N. Arnold and S. Bauer, *Proc. Natl. Acad. Sci.*, 2010, **107**, 4505–4510.
7 S. J. A. Koh, X. Zhao and Z. Suo, *Appl. Phys. Lett.*, 2009, **94**, 262902.
8 S. J. A. Koh, C. Keplinger, T. Li, S. Bauer and Z. Suo, *IEEE/ASME Transactions on Mechatronics*, 2011, **16**, 33–41.
9 J. Huang, S. Shian, Z. Suo and D. R. Clarke, *Adv. Funct. Mater.*, 2013, **23**, 5056–5061.
10 R. Kaltseis, C. Keplinger, S. J. A. Koh, R. Baumgartner, Y. F. Goh, W. H. Ng, A. Kogler, A. Tröls, C. C. Foo and Z. Suo, *et al.*, *RSC Adv.*, 2014, **4**, 27905–27913.
11 S. Bauer, S. Bauer-Gogonea, I. Graz, M. Kaltenbrunner, C. Keplinger and R. Schwödiauer, *Adv. Mater.*, 2014, **26**, 149–162.
12 Q. Deng, L. Liu and P. Sharma, *Journal of the Mechanics and Physics of Solids*, 2014, **62**, 209–227.
13 Q. Deng, L. Liu and P. Sharma, *Phys. Rev. E: Stat., Nonlinear, Soft Matter Phys.*, 2014, **90**, 012603.
14 K. Stark and C. Garton, *Nature*, 1955, **176**, 1225–1226.
15 J.-S. Plante and S. Dubowsky, *Int. J. Solids Struct.*, 2006, **43**, 7727–7751.
16 X. Zhao and Z. Suo, *Appl. Phys. Lett.*, 2009, **95**, 031904.
17 X. Zhao and Z. Suo, *Phys. Rev. Lett.*, 2010, **104**, 178302.
18 Q. Wang, L. Zhang and X. Zhao, *Phys. Rev. Lett.*, 2011, **106**, 118301.

19 Q. Wang and X. Zhao, *Phys. Rev. E: Stat., Nonlinear, Soft Matter Phys.*, 2013, **88**, 042403.
20 S. Ashley, *Sci. Am.*, 2003, **289**, 52–59.
21 P. Brochu and Q. Pei, *Macromol. Rapid Commun.*, 2010, **31**, 10–36.
22 S. Yang, K. Khare and P.-C. Lin, *Adv. Funct. Mater.*, 2010, **20**, 2550–2564.
23 Q. Wang, D. Robinson and X. Zhao, *Appl. Phys. Lett.*, 2014, **104**, 231605.
24 C. Keplinger, T. Li, R. Baumgartner, Z. Suo and S. Bauer, *Soft Matter*, 2012, **8**, 285–288.
25 T. Li, C. Keplinger, R. Baumgartner, S. Bauer, W. Yang and Z. Suo, *Journal of the Mechanics and Physics of Solids*, 2013, **61**, 611–628.
26 X. Zhao and Q. Wang, *Applied Physics Reviews*, 2014, **1**, 021304.
27 N. Hu and R. Burgueño, *Smart Mater. Struct.*, 2015, **24**, 063001.
28 X. Zhao and Z. Suo, *Appl. Phys. Lett.*, 2007, **91**, 061921.
29 S. M. Ha, W. Yuan, Q. Pei, R. Pelrine and S. Stanford, *Adv. Mater.*, 2006, **18**, 887–891.
30 X. Niu, H. Stoyanov, W. Hu, R. Leo, P. Brochu and Q. Pei, *Journal of Polymer Science Part B: Polymer Physics*, 2013, **51**, 197–206.
31 B. Li, J. Zhou and H. Chen, *Appl. Phys. Lett.*, 2011, **99**, 244101.
32 G. Kofod, *J. Phys. D: Appl. Phys.*, 2008, **41**, 215405.
33 S. Akbari, S. Rosset and H. R. Shea, *Appl. Phys. Lett.*, 2013, **102**, 071906.
34 L. Jiang, A. Betts, D. Kennedy and S. Jerrams, *J. Phys. D: Appl. Phys.*, 2016, **49**, 265401.
35 Z. Suo, X. Zhao and W. H. Greene, *Journal of the Mechanics and Physics of Solids*, 2008, **56**, 467–486.
36 S. Yang, X. Zhao and P. Sharma, *J. Appl. Mech.*, 2017, **84**, 031008.
37 L. Dorfmann and R. W. Ogden, *International Journal of Engineering Science*, 2014, **77**, 79–101.
38 R. Pelrine, R. Kornbluh, Q. Pei and J. Joseph, *Science*, 2000, **287**, 836–839.
39 S. Shian, J. Huang, S. Zhu and D. R. Clarke, *Adv. Mater.*, 2014, **26**, 6617–6621.